# Generalized pseudo-Anosov maps arising from holomorphic dynamics

by

Mariam Al-Hawaj

A thesis submitted in conformity with the requirements
for the degree of Doctor of Philosophy

Department of Mathematics
University of Toronto

Generalized pseudo-Anosov maps arising from holomorphic dynamics

Mariam Al-Hawaj
Doctor of Philosophy

Department of Mathematics
University of Toronto
2024

# Abstract

In this thesis, we develop a new connection between the dynamics of quadratic polynomials on the complex plane and the dynamics of homeomorphisms of surfaces. In particular, given a quadratic polynomial, we investigate whether one can construct an extension of it which is a generalized pseudo-Anosov homeomorphism. Generalized pseudo-Anosov means it preserves a pair of foliations with infinitely many singularities that accumulate on finitely many points. We determine for which quadratic polynomials such an extension exists. The construction is related to the dynamics on the Hubbard tree, which is a forward invariant subset of the filled Julia set containing the critical orbit. We define a type of Hubbard trees, which we call crossing-free, and show that these are precisely the Hubbard trees for which one can construct a generalized pseudo-Anosov map.

To my mother Zahra Al-Khawaja and my late father Yousif Al-Hawaj.

# Acknowledgements

First and foremost, I would like to extend my sincere thanks to my supervisor, Giulio Tiozzo, for his continuous help and support throughout my PhD studies. His dedication, time, and effort in introducing me to a wide range of problems and topics have been instrumental in shaping this thesis. This work would not have been possible without his guidance.

I am thankful to Charmaine C. Williams, the former Vice Dean of the School of Graduate Studies at the University of Toronto, to Regina Rotman, my mentor, to Kumar Murty, and to Ilia Binder, my master's supervisor for their invaluable guidance and support. I am also thankful to my friends Zohreh Shehbazi, Janane Krayem, and Esme Tremblay, for their companionship and encouragement along the way.

I am grateful to all the researchers who supported my work and invited me to give talks at their institutions, including Pierre Arnoux, Rebecca Winarski, Dan Margalit, Boris Hasselblatt, Kathryn Lindsey, Daniel Groves, and Kevin Pilgrim. I also appreciate Ethan Farber and Chenxi Wu for helpful discussions and their shared insights.

I extend my heartfelt gratitude to my family. To my mother Zahra, whose patience and prayers have been a source of strength throughout this journey. To my siblings Jawad, Abdullah, A. Majeed, A. Wahab, Anisa, Badria, Mona, Hussein and Ahmed for their continuous support and encouragement.

Finally, I want to thank my husband, Anwar Hashim, and my two wonderful daughters, Noor and Yosra, for their love and support.

Thank you all for your significant contributions and support.

# Contents

# Chapter 1

# Introduction

## 1.1 Motivation

The interplay of geometric topology and complex dynamics has proved to be fruitful, at least since the work of Thurston, and there have been recently new developments. The goal of this thesis lies at the intersection of both fields in order to develop new connections between the two areas.

The Nielsen-Thurston classification [FM12] of mapping classes established that every orientation preserving homeomorphism of a closed surface, up to isotopy, is either periodic, reducible, or pseudo-Anosov. Pseudo-Anosov maps have particulary nice structure because they expand along one foliation by a factor of $\lambda > 1$ and contract along a transversal foliation by a factor of $\frac{1}{\lambda}$. The number $\lambda$ is called the *dilatation* of the pseudo-Anosov.

Fried showed [Fr85] that every dilatation $\lambda$ of a pseudo-Anosov map is an algebraic unit, and conjectured that every algebraic unit $\lambda$ whose Galois conjugates lie in the annulus $A_\lambda = \{z : \frac{1}{\lambda} < |z| < \lambda\}$, known as *bi-Perron* unit, is a dilatation of some pseudo-Anosov on some surface $S$.

Moreover, the dilatation $\lambda_\varphi$ of the pseudo-Anosov $\varphi$ measures the dynamical complexity of the pseudo-Anosov map. Precisely, the topological entropy of the pseudo-Anosov equals $\log \lambda_\varphi$, see [BCK21]. Thurston [Th14] proved that a positive real number $h$ is the topological entropy of a *post-critically finite (PCF)* self-map of the unit interval if and only if $\lambda = \exp(h)$ is *weak Perron*. A weak Perron number is an algebraic integer $\lambda$ that is at least as large as the absolute value of any of its Galois conjugates.

Pseudo-Anosovs play a huge role in Teichmüller theory and geometric topology. The relation between these and complex dynamics has been well studied, inspired by Thurston.

Thurston's theory uses train tracks and their endomorphisms to combinatorially describe pseudo-Anosov maps of surfaces. Train tracks [PH91] are graphs embedded in the surface equipped with additional data on their vertices that specifies how to "turn" and "follow" along the tracks. Then the

associated Markov matrix gives enough information to reconstruct the surface by building rectangles with sides parallel to the horizontal and vertical foliations and then gluing them. Then following the train track map, the pseudo-Anosov stretches these rectangles horizontally and contracts them vertically.

Constructing pseudo-Anosov maps has been an active area of research for many decades starting with Penner [Pe88] and Thurston [Th88] up to the more recent work of Hubbard, Rafiqi and Schang, where they constructed pseudo-Anosovs from permutations and matrices [HRS19].

Following the steps of Thurston's theory on train tracks, de Carvalho-Hall and Farber constructed generalized pseudo-Anosovs from real quadratic polynomials [dCH04] [Fa22]. Generalized pseudo-Anosov maps are similar to pseudo-Anosovs except that the invariant foliations are allowed to contain infinitely many singularities provided that they accumulate at finitely many points. In their work, train tracks are still finite graphs with endomorphisms that are still finite to one, however, they are allowing the additional information on vertices to be infinite. The question then arises if one can generalizes this to complex, instead of real, polynomials

The goal of this thesis is to build a new connection between complex dynamics and Teichmüller theory by constructing *generalized pseudo-Anosov* maps of surfaces from polynomials acting on the complex plane. The construction will be related to the dynamics on the Hubbard tree $T$, which is an invariant subset of the filled Julia set (see Section 2.5 for the definition). So basically, we are interested in the following question.

*Question* 1.1.1. If $f : T \to T$ is a post-critically finite quadratic polynomial with Hubbard tree $T$, is there a surface $S$ and a generalized pseudo-Anosov homeomorphism $\varphi : S \to S$ that is an extension of $f$?

$$\begin{array}{ccc} S & \xrightarrow{\varphi} & S \\ {\scriptstyle\pi}\downarrow & & \downarrow{\scriptstyle\pi} \\ T & \xrightarrow{f} & T \end{array}$$

In other words, we require the above diagram to commute.

## 1.2 Main result

We will show that the type of Hubbard trees for which the construction is possible are those that are crossing-free and non-degenerate.

A Hubbard tree is *non-degenerate* when the critical point is not an endpoint: thus, it divides the tree into two sub-trees. We call *upper branch* $B_u$ the sub-tree containing the critical value, and *lower branch* $B_l$ the other one.

**Definition 1.2.1.** A Hubbard tree $T$ is said to be *crossing-free* if there exists an embedding of $T$ into the plane $\mathbb{C}$ that satisfies the following:

The image $f(B_l)$ of the lower branch can be isotoped, while fixing the endpoints of $T$, into a tree that does not intersect the interior of the image $f(B_u)$ of the upper branch.

Below are examples of both a crossing-free Hubbard tree and a Hubbard tree with crossing.

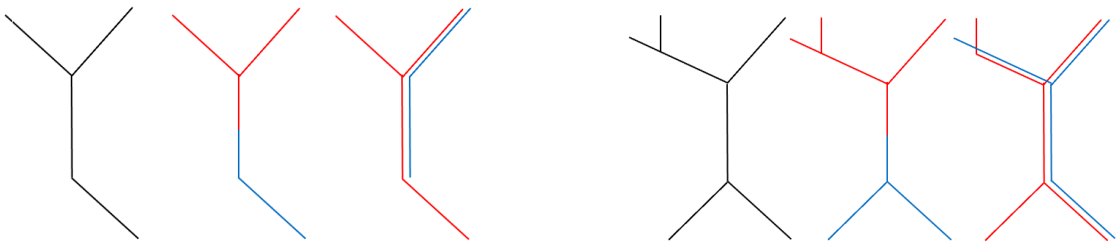

Crossing-free Hubbard tree. Hubbard tree with crossing.

Figure 1.1: Examples of Hubbard trees.

**Definition 1.2.2.** Let $T$ be the Hubbard tree of a post-critically finite quadratic polynomial. We say that $f$ is *extendable* to a generalized pseudo-Anosov homeomorphism if there exist a surface $S$ and a generalized pseudo-Anosov $\varphi$ such that $\varphi$ is an extension of $f$.

The main result of this paper is the following:

**Theorem 1.2.3.** *Let $f$ be a superattracting quadratic polynomial and let $T$ be its Hubbard tree. Then $(f, T)$ is extendable to a generalized pseudo-Anosov if and only if it is crossing-free.*

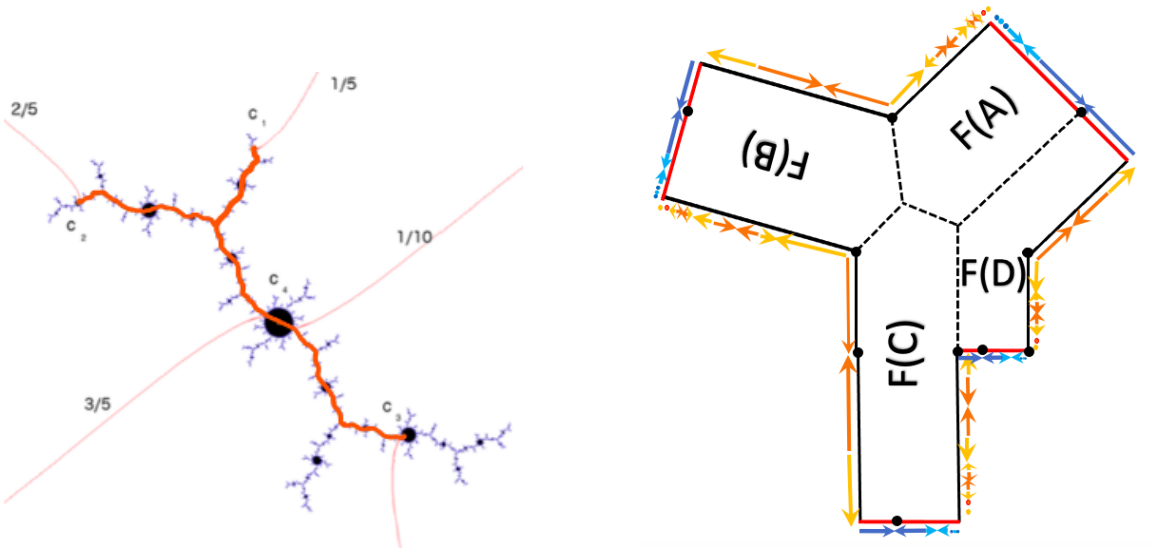


Crossing-free Hubbard tree. Generalized pseudo-Anosov map.

Figure 1.2: The correspondence from Theorem 1.2.3.

Note that the dilatation $\lambda$ of the generalized pseudo-Anosov satisfies $\lambda = \exp(h(f))$ where $h(f)$ denotes the *core entropy* of the polynomial $f$.

This result generalizes to complex polynomials the results of de Carvalho-Hall and Farber, who constructed generalized pseudo-Anosovs from real quadratic polynomials [dCH04] [Fa22].

To give an idea of the proof, the construction of the pseudo-Anosov map, that we will see in Section 5.1, goes as follows:

1. First, we thicken the tree and then we define a *thick map* on it.
2. Since the map folds the thickened tree and to keep track of the folding, we construct a *tree-like train track* by a procedure that's shown in Figure 5.3.
3. We then use the dynamics of the train track to compute the transition matrix whose leading eigenvalue will be our dilatation $\lambda$.
4. Moreover, we use the eigenvectors of the matrix as the dimensions of the rectangles that we build.
5. After that, we identify the rectangles to create the generalized pseudo-Anosov homeomorphism.

To prove the converse (Theorem 5.1.11), we use the invariant foliation of the generalized pseudo-Anosov to isotope apart the upper and the lower branches showing that the Hubbard tree must be crossing-free.

## 1.3 Further questions

This thesis opens up several areas of investigation. For instance, one may consider the following questions:

1. Is there a classification of generalized pseudo-Anosovs? See also the recent thesis [Di24].
2. For which parameters in the Mandelbrot set the above construction is possible? In other words, which quadratic Hubbard trees are crossing-free? Probably, this corresponds exactly to parameters in the principal veins.
3. Determine which algebraic numbers give rise to entropies of these generalized pseudo-Anosovs in the spirit of Fried's conjecture.
4. Given a value of the entropy $h = \log(\lambda)$, can it be realized as the core entropy of *both* a real PCF quadratic polynomial and a PCF polynomial on a principal vein?
5. Can we extend Theorem 1.2.3 to any post-critically finite polynomial, i.e. to the polynomials for which the orbit of the critical point is pre-periodic?

The thesis is made up of six chapters. Chapter 2 contains the background needed from complex dynamics, while Chapter 3 contains preliminaries from geometric topology. In Chapter 4 we will introduce new tools that we will need in our proof of the main result. Chapter 5 shows the proof of the main theorem (Theorem 5.1), and finally, in Chapter 6 we discuss a detailed example of the construction of a generalized pseudo-Anosov map.

# Chapter 2

# Complex Dynamics

In this chapter, we will provide the background needed from complex dynamics. Our work will be related to quadratic polynomials acting on the complex plane $\mathbb{C}$. But first, we will start with preliminaries of the dynamics of iterated holomorphic mappings from a Riemann surface to itself.

## 2.1 Riemann surfaces

A*Riemann surface* is a connected complex analytic manifold of complex dimension one. By the uniformization theorem, a simply connected Riemann surface is conformally isomorphic to one of the following:

1. the complex plane $\mathbb{C}$,
2. the open unit disk $D \subset \mathbb{C}$, or
3. the Riemann sphere $\hat{\mathbb{C}} = \mathbb{C} \cup \{\infty\}$.

These Riemann surfaces are distinct because $\hat{\mathbb{C}}$ is the only compact one and any holomorphic map $\mathbb{C} \to D$ is constant by the Liouville's Theorem.

## 2.2 Periodic points

Let $S$ be a Riemann surface, and $f : S \to S$ be a holomorphic map.

A *periodic point* of $f$ is a point $z$ such that $f^{\circ p}(z) = z$, where $f^{\circ p}$ is the $p$-th iteration of $f$. The smallest such $p$ is called the *period* of $z$. The set

$$\{z, f(z), f^{\circ 2}, \ldots, f^{\circ p}(z) = z\}$$

is called the *periodic orbit* or *cycle*. If the Riemann surface $S \subseteq \mathbb{C}$, then the derivative $\lambda = (f^{\circ p})'(z)$ is a well-defined complex number. $\lambda$ is called the *multiplier* of the periodic orbit. In general, if $S$ is any arbitrary Riemann surface, we can define the multiplier using a local coordinate chart around any point of the orbit.

Periodic orbits are classified, according to the multiplier $\lambda$, as either:

- **attracting** if $|\lambda| < 1$, and **superattracting** if $\lambda = 0$,
- **repelling** if $|\lambda| > 1$, or
- **indifferent (neutral)** if $|\lambda| = 1$.

A periodic orbit is called *rationally indifferent* or *parabolic* if $\lambda = e^{2\pi \frac{p}{q} i}$ for some $\frac{p}{q} \in \mathbb{Q}$.

## 2.3 Mandelbrot and Julia sets

Consider the family of quadratic polynomials $f_c(z) := z^2 + c$, where both $z$ and $c$ are in the complex plane $\mathbb{C}$. We call the $c-$plane the *parameter plane* and the $z$-plane the *dynamic plane*. For each parameter $c$, $f_c$ has a unique critical point $z = 0$. Moreover, to each parameter $c$ in the parameter plane, there corresponds the critical value $f_c(0) = c$ in the dynamic plane. We recall the following definitions where we refer to [DH84] for more details:

**Definition 2.3.1.** The *filled Julia set* $K(f_c)$ of $f_c$ is given by

$$K(f_c) := \{z \in \mathbb{C} : f_c^n(z) \not\to \infty\},$$

i.e. it is the union of all bounded orbits.

**Definition 2.3.2.** The *Julia set* $J(f_c)$ of $f_c$ is the boundary of the filled Julia set, i.e. $J(f_c) := \partial K(f_c)$. The complement of the Julia set is called the *Fatou set*, and its connected components are called *Fatou components.*

**Definition 2.3.3.** The *Mandelbrot set* $M$ is given by

$$M := \{c \in \mathbb{C} : J(f_c) \text{ is connected}\}.$$

Moreover, the parameter $c \in M$ if and only if the critical orbit is bounded, i.e. if and only if $0 \in K(f_c)$. Let $M'$ be the set of parameters $c$ for which $f_c$ has an attracting cycle. The connected components of $M'$ are called the *hyperbolic components* of $\overset{\circ}{M}$.

## 2.4 External rays

The complement of the Mandelbrot set is a non-empty, open set, and simply connected in the Riemann sphere $\hat{\mathbb{C}}$. Consider the unique Riemann map $\Phi : \mathbb{C}\backslash\bar{\mathbb{D}} \to \mathbb{C}\backslash M$ with $\Phi(\infty) = \infty$ and $\Phi^{'}(\infty) > 0$. We can define external rays as follows:

**Definition 2.4.1.** For $\theta \in \mathbb{R}/\mathbb{Z}$, we define the *external ray at* $\theta$ to be the set $R_M(\theta) := \Phi(\{\rho e^{2\pi i\theta},\ \rho > 1\})$. An external ray $R_M(\theta)$ is said to *land at* $x$ if

$$\lim_{\rho \to 1^+} \Phi(\rho e^{2\pi i\theta}) = x.$$

In [DH84], it's shown that every external ray of $M$ with rational angle lands.

If the rational angle in the reduced form is $\theta = \frac{p}{q}$, then there are two cases for the point $c$ where the external ray lands:

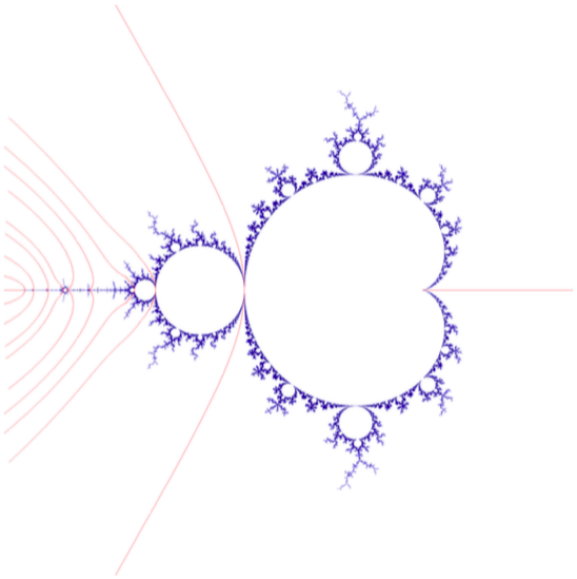

Figure 2.1: External rays.

- **Case 1.** When the denominator $q$ is odd, then the external ray $R_M(\theta)$ lands on a parameter $c$ such that $f_c$ has rationally indifferent orbit. In this case, two external rays land at such point $c$, except for the parameter $c = \frac{1}{4}$ where only the external ray of angle $\theta = 0$.
- **Case 2.** When the denominator $q$ is even, then the external ray $R_M(\theta)$ lands on a parameter $c$ such that the critical orbit of $f_c$ falls on a repelling orbit. Such parameter $c$ is called *Misurewicz* point. Each Misurewicz point has finitely many external rays landing on it.

For each component $U$ of $M'$ and for each $c \in U$, $f_c$ has a unique attracting cycle of some period $p$. Let $z_c$ be a point in the cycle. The map $\varphi_U : U \to \mathbb{D}$ given by $\varphi_U(c) := (f^{\circ p})'(z_c)$ is a conformal mapping which extends injectively to the boundary. We define the *center* of $U$ to be $\varphi_U(c)^{-1}(0)$ and the *root* of $U$ to be $\varphi_U(c)^{-1}(1)$.

## 2.5 Hubbard trees

**Definition 2.5.1.** A polynomial $f : \mathbb{C} \to \mathbb{C}$ is said to be *post-critically finite* if the forward orbit of every critical point of $f$ is finite.

Recall a rational angle $\theta \in \mathbb{Q}/\mathbb{Z}$ determines a post-critically finite map $f_\theta(z) := z^2 + c_\theta$. If $\theta$ is pre-periodic for the doubling map, then the external ray of angle $\theta$ lands at a post-critically finite parameter that we denote as $c_\theta$. If $\theta$ is purely periodic for the doubling map, then the external ray lands at the root of a hyperbolic component, and we let $c_\theta$ be the centre of such component.

*Remark* 2.5.2. If f is post-critically finite, then the filled Julia set $K(f)$ is connected and locally connected. This implies that $K(f)$ is path-connected. Moreover, If $f$ is post-critically finite, then there are two cases for $f$:

- $f$ is Misiurewicz. This means that the critical points of $f$ are strictly pre-periodic. In this case, the interior of the filled Julia set $K(f)$ of $f$ is empty. Therefore, for any two points $x, y \in K(f)$, there exist a unique arc between them.

- $f$ is super-attracting. This is the case when critical points are purely periodic. In this case, for every bounded Fatou component $U$, there exists (up to rotation) a unique biholomorphism $\varphi_u : U \to \mathbb{D}$. For a fixed angle $\theta$, we call $\{\varphi_u(re^{2\pi\theta i}) : 0 \leq r \leq 1\}$ a *radial arc* of $U$.

**Definition 2.5.3.** An arc $I$ inside the filled Julia set is said to be *regulated* if the intersection of $I$ with the closure of every bounded Fatou component is either empty, a point, or a union of radial arcs.

We are ready now to define the Hubbard tree.

**Definition 2.5.4.** Let $f$ be a post-critically finite quadratic polynomial with critical point $c_0$ and let $c_i = f^{\circ i}(c_0)$. We define the *Hubbard tree* $T$ of $f$ to be the union of the regulated arcs

$$T = \bigcup_{n,m\geq 0} [c_n, c_m].$$

It is a forward invariant subset of the filled Julia set $K(f)$ that contains the critical orbit.

**Example 2.5.5.** Let $f$ be a quadratic polynomial with the characteristic angle $\theta = \frac{1}{5}$. Then the critical point $c_0$ has period $p = 4$. Then looking at the Julia set of $f$, in Figure 2.2, we can see the Hubbard tree which is the union of the regulated arcs $[c_1, c_3]$ and $[c_2, c_3]$. Also we can see the external rays that land at the roots of the Fatou components containing the elements of the critical orbit. Note that the angles $\frac{\theta}{2} = \frac{1}{10}$ and $\frac{\theta+1}{2} = \frac{3}{5}$ both land on the boundary of the critical Fatou component containing the point $c_0 = c_4$.

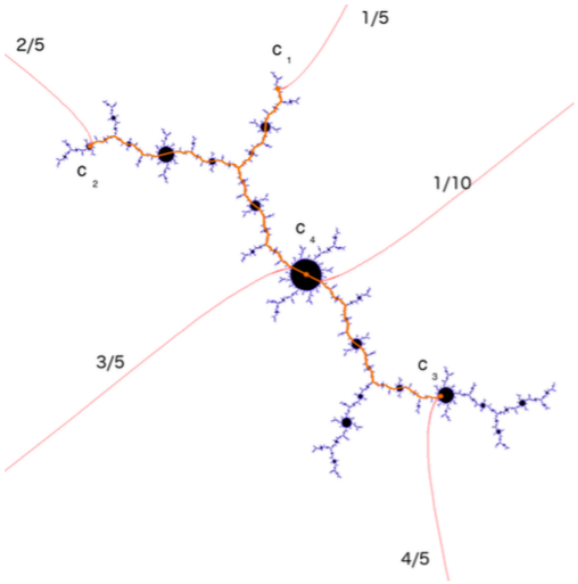


Figure 2.2: Hubbard tree for post-critically finite quadratic polynomial with angle $\theta = \frac{1}{5}$, and $p = 4$.

## 2.6 Core entropy

The topological entropy of a continuous real map is a measure of the dynamical complexity of the map. In particular, it is the measure of the complexity of the orbits of the map. It is defined to be

the growth rate of different orbits of length $n$. Let $(X, d)$ be a compact metric space and $f : X \to X$ is a continuous map. A set $E \subseteq X$ is said to $(n, \epsilon)$-span another set $K$ if for each $x \in K$ there exists $y \in E$ such that $d(f^{\circ i}(x), f^{\circ i}(y)) \leq \epsilon$ for all $0 \leq i \leq n$, i.e. if every point of $K$ stays close to some point in $E$ for the first $n$ iterates. If $K \subseteq X$ is compact, we let $N(n, \epsilon, K)$ be the minimal cardinality of all $E \subseteq K$ that $(n, \epsilon)$-spans K. We define the topological entropy as follows [Ti15]:

**Definition 2.6.1.** Let $f : X \to X$ be a continuous map on a compact metric space, and let $K \subseteq X$. The topological entropy of $f$ with respect to $K$ is defined by

$$h_{top}(f, K) = \lim_{\epsilon \to 0} \lim_{n \to \infty} \frac{1}{n} \log N(n, \epsilon, K).$$

Moreover, the topological entropy of $f$ is defined by

$$h_{top}(f) = h_{top}(f, X).$$

W. Thurston [Th14] [TBGHLLT22] introduced the core entropy of post-critically finite complex polynomial as follows:

**Definition 2.6.2.** The *core entropy* $h(f)$ of a post-critically finite polynomial $f$ is defined to be the topological entropy of the restriction of $f$ to its Hubbard tree $T$,

$$h(f) := h_{top}(f, T).$$

If $\theta$ is a rational number, we consider the associated quadratic polynomial $f_\theta$ as

$$h(\theta) := h(f_\theta).$$

## 2.7 Lamination

Julia sets and the Mandelbrot set can have topological models given by *lamination*. They represent equivalence relations on the boundary $\partial\bar{\mathbb{D}}$ of the disk arising from external rays landing on the same point. *lamination* are defined as follows:

**Definition 2.7.1.** A *geodesic lamination* $L$ is a closed set of disjoint union of hyperbolic geodesics called *leaves* in the closed unit disk $\bar{\mathbb{D}}$.

A *gap* of a lamination $L$ is the closure of a component of the complement of the union of all leaves.

Julia sets of quadratic polynomials can be modeled by *invariant quadratic laminations*. The action of the map $f(z) = z^2$ on the boundary of the unit disk induces a dynamics on the lamination $L$ as follows: The image of a leaf $\overline{ab}$ with endpoints $a$ and $b$ is the leaf of the images $f(a)$ and $f(b)$ of the endpoints, i.e.

$$f(\overline{ab}) := \overline{f(a)f(b)}.$$

A leaf of maximal length in a lamination is called a *major leaf*, and its image a *minor leaf*. A quadratic invariant lamination has two major leaves, and a unique minor leaf. An equivalence

relation $\sim$ on the boundary of the unit disk as follows: $\theta_1 \sim \theta_2$ if the rays $R_c(\theta_1)$ and $R_c(\theta_2)$ land on the same point.

To construct a model for the Mandelbrot set, Thurston defined the *quadratic minor lamination* $L_{QM}$ to be the union of the minor leaves of all quadratic invariant laminations. See [Th09] and figure 2.3.

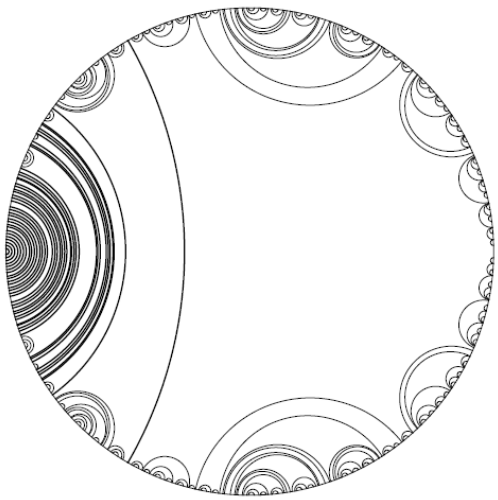

Figure 2.3: A topological model for M by Lamination.

## 2.8 Veins

In parameter space, a *vein* is a generalization of the real slice, $\mathbb{R} \cap M$. A vein $v$ is an embedded arc in $M$, joining a parameter $c \in \partial M$ with the center of the main cardioid. The following definitions are taken from [Ti15]:

**Definition 2.8.1.** Given a vein $v$ and a parameter $c$ on $v$, we can define the set $R_c$ as the set of external angles of rays which land on $v$ closer than $c$ to the main cardioid:

$$R_c := \{\theta \in S^1 : R_M(\theta) \text{ lands on } v \cap [0, c]\}$$

where $[0, c]$ means the segment of vein joining $c$ to the center of the main cardioid.

In the $\frac{p}{q}$-limb, there is a unique parameter $c_{\frac{p}{q}}$ such that the critical point lands on the $\beta$ fixed point after $q$ iterates (i.e. $f^{\circ q}(0) = \beta$).

A *vein* in the Mandelbrot set is a continuous, injective arc inside the Mandelbrot set $M$. Now we define veins combinatorially just in terms of laminations as follows: The degenerate leaf $\{0\}$ is the natural root of quadratic minor lamination $L_{QM}$. No other leaf of $L_{QM}$ contains the angle 0 as its endpoint. Given a rooted lamination, we define a *partial order* on the set of leaves by saying that $l_1 < l_2$ if $l_1$ separates $l_2$ from the root.

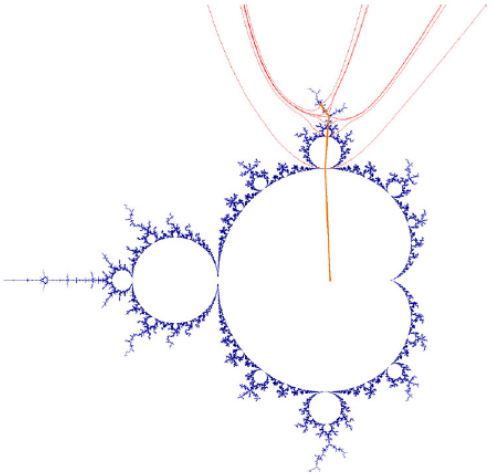

Figure 2.4: A vein joining the center of the main cardioid with the main antenna in the $\frac{1}{3}$-limb ($\theta = \frac{1}{4}$), and external rays landing on it.

**Definition 2.8.2.** Let $l$ be a minor leaf. Then the *combinatorial vein* defined by $l$ is the set

$$P(l) := \{l' \in L_{QM} : \{0\} < l' < l\}$$

of leaves which separate $l$ from the root of the lamination.

## 2.9 Principal vein

Let $\frac{p}{q}$ be a rational number, with $0 < p < q$ and $p, q$ coprime. The $\frac{p}{q}$-limb in the Mandelbrot set is the set of parameters which have rotation number $\frac{p}{q}$ around the $\alpha$ fixed point. In each limb, there exists a unique parameter $c = c_{\frac{p}{q}}$ such that the critical point maps to the $\beta$ fixed point after exactly $q$ steps, i.e. $f_c^{\circ q}(0) = \beta$. These parameters represent the "highest antennas" in the limbs of the Mandelbrot set.

**Definition 2.9.1.** The *principal vein* $v_{\frac{p}{q}}$ is the vein joining $c_{\frac{p}{q}}$ to the main cardioid. We shall denote by $\theta_{\frac{p}{q}}$ the external angle of the ray landing at $c_{\frac{p}{q}}$ in parameter space.

Figure 2.4 shows the vein joining the center of the main cardioid with the main antenna in the $\frac{1}{3}$-limb ($\theta = \frac{1}{4}$), and external rays landing on it. For more details, see [DH84].

# Chapter 3

# Geometric Topology

In this chapter, we will provide a brief background from geometric topology. We consider a surface $S$ which is a 2-dimensional manifold, with two fundamental objects attached to it: a group and a space. We will mainly recall the definitions and main classifications of the former object, that is the group.

## 3.1 Mapping class group

A group of interest in geometric topology is the *mapping class group* of a surface $S$, denoted by $Mod(S)$, which is defined as the group of isotopy classes of orientation preserving homeomorphisms of $S$.

### 3.1.1 Periodic mapping classes

A periodic mapping class $f$ is a finite order element in $Mod(S)$. This is equivalent to $f$ having an automorphism of a Riemann surface as representative. Moreover, each periodic element of $Mod(S)$ can be realized as an isometry of $S$ with respect to some hyperbolic metric.

### 3.1.2 Reducible mapping classes

An element $f$ of $Mod(S)$ is reducible if there is a nonempty set $\{c_1, \ldots, c_n\}$ of isotopy classes of essential simple closed curves in $S$ such that $i(c_i, c_j) = 0$ for all $i$ and $j$ and so that $\{f(c_i)\} = c_i$ for $i = 1, \ldots, n$. An example of a reducible mapping class is a Dehn twist $T_a$. Another example is the mapping class given in Figure 3.1. This shows that there is an overlap between the set of periodic and reducible elements of $Mod(S)$.

### 3.1.3 Pseudo-Anosov mapping classes

**Definition 3.1.1.** An element $f$ of $Mod(S)$ is said to be *pseudo-Anosov* if there is a pair of transverse measured foliations $(\mathcal{F}^u, \mu^u)$ and $(\mathcal{F}^s, \mu^s)$ on $S$, a number $\lambda > 1$, and a representative homeomorphism $\varphi : S \to S$ such that the following hold:

$$\varphi_*(\mathcal{F}^u, \mu^u) = (\mathcal{F}^u, \lambda\mu^u) \text{ and } \varphi_*(\mathcal{F}^s, \mu^s) = (\mathcal{F}^s, \frac{1}{\lambda}\mu^s).$$

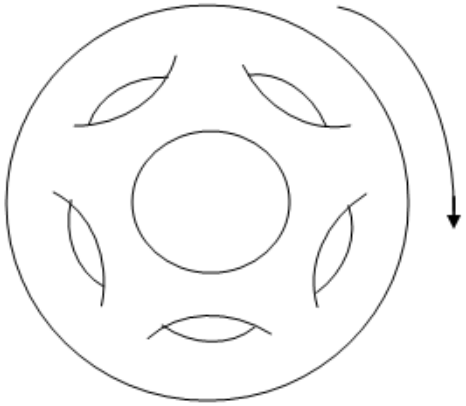

Figure 3.1: Periodic mapping Class.

The measured foliations $(\mathcal{F}^u, \mu^u)$ and $(\mathcal{F}^s, \mu^s)$ are called the *unstable foliation* and the *stable foliation*, and the number $\lambda$ is called the *dilatation* of $\varphi$.

### 3.1.4 Classification

We recall the celebrated Nielsen–Thurston classification:

**Theorem 3.1.2.** *Let $g, n \geq 0$. Each mapping class $f \in Mod(S_{g,n})$ is periodic, reducible, or pseudo-Anosov. Further, pseudo-Anosov mapping classes are neither periodic nor reducible.*

## 3.2 Generalized pseudo-Anosov mapping classes

The following definition of generalized pseudo-Anosov map is taken from [dCH04]:

**Definition 3.2.1.** A homeomorphism $\varphi : S \to S$ of a smooth surface $S$ is called a *generalized pseudo-Anosov* map if there exist

1. a finite $\varphi-$invariant set $\Sigma$;
2. a pair $(\mathcal{F}^u, \mu^u),\ (\mathcal{F}^s, \mu^s)$ of transverse measured foliations of $S\backslash\Sigma$ with *countably many pronged singularities*, which accumulate on each point of $\Sigma$ and have no other accumulation points;
3. a real number $\lambda > 1$; such that

$$\varphi(\mathcal{F}^u, \mu^u) = (\mathcal{F}^u, \lambda\mu^u) \text{ and } \ \varphi(\mathcal{F}^s, \mu^s) = (\mathcal{F}^s, \frac{1}{\lambda}\mu^s).$$

## 3.3 Train-tracks

The following definition of train tracks is taken from [PH91]:

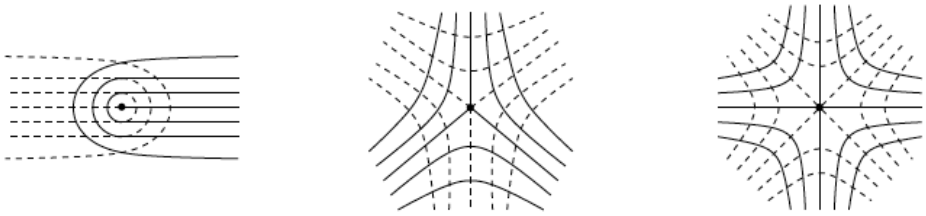

Figure 3.2: Pronged singularities of the invariant foliations.

**Definition 3.3.1.** Let $\tau \subset S$ be a finite collection of one-dimensional CW complexes, each made up of vertices, called switches, and edges, called branches, disjointly embedded in $S$. We say that $\tau \subset S$ is a *train track* in $S$ provided that the following conditions hold:

1. (Smoothness) $\tau$ is $C^1$ away from its switches,

2. (Non-degeneracy) For any switch $v$ of $\tau$, there is an embedding $f : (0, 1) \to \tau$ with $f(\frac{1}{2} = v$ which is a $C^1$ map into $S$. So no switch of $\tau$ is univalent, and we moreover demand that each simple closed curve component of $\tau$ contains a unique bivalent switch and that every other switch of $\tau$ is at least trivalent,

3. (Geometry) Suppose that $F$ is a component of $S - \tau$, and let $D(F)$ denote the double of $F$ along the $C^l$ frontier edges of $F$. Thus, non-smooth points in the frontier of $F$ give rise to punctures of $D(F)$. We require that the Euler characteristic $\chi(D(F))$ of $D(F)$ be negative.

# Chapter 4

# New Tools

We now introduce two new mathematical objects that are useful for our construction.

## 4.1 Thick Hubbard trees

**Definition 4.1.1.** We define an *n-star* $X$ to be a topological space homeomorphic to a disc with $2n$ marked points on the boundary denoted in counter-clockwise order as $p_i, i = 1, \dots, 2n$. We define the *inner boundary* $\partial_{in}X$ of $X$ as the subset of the boundary of $X$ given by the union of the arcs

$$\partial_{in}X = \bigcup_{i=1}^{n} [p_{2i-1}, p_{2i}].$$

Similarly, we define the *outer boundary* $\partial_{out}X$ of $X$ as the union

$$\partial_{out}X = \bigcup_{i=1}^{n} [p_{2i}, p_{2i+1}]$$

where $p_{2n+1} = p_1$. We call a 2-star a *rectangle*.

We now give the definition of thick tree:

**Definition 4.1.2.** A *thick tree* is a closed topological 2-disc $\mathbb{T}$ consisting of junctions, sides.

*Junctions* are homeomorphic to a closed 2-disc and are of two types: *end-junctions* and *inner-junctions* (representing the vertices and the post-critical set of the Hubbard tree, respectively). The boundary of the junctions are divided into two parts. One part intersects the boundary of the thick tree and the other part intersects the boundary of a side.

*Sides* are $n$-stars; moreover, every component of their inner boundary is contained in the boundary of a junction, and every component of their outer boundary is contained in the boundary of $\mathbb{T}$. For $n = 2$, they are called *simple sides* and represent the thickening of the edges of the Hubbard tree. For $n > 2$, $n$-stars represent a thickening of a neighbourhood of an $n$-valence branch point in the Hubbard tree.

**Definition 4.1.3.** We say that the $n$-star $X$ *connects* the junctions $J_1, \dots, J_k$ if the components of the inner boundary of $X$ are contained in the boundary of the junctions $J_1, \dots, J_k$.

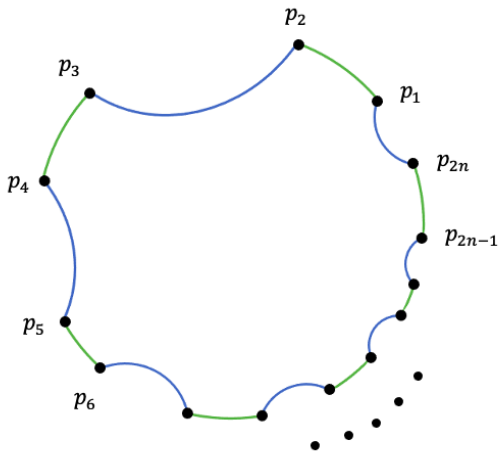


Figure 4.1: $n$-star.

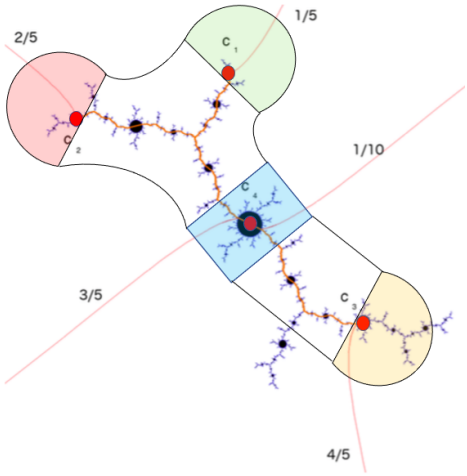


Figure 4.2: Thick Hubbard tree.

Figure 4.2 shows a thick Hubbard tree with four junctions (blue, green, red, yellow), one 3-star (connecting the blue, green, and red junctions), and one simple side (connecting the blue and yellow junctions).

## 4.2 Thick tree maps

We define a map on the thick tree $\mathbb{T}$ as follows:

**Definition 4.2.1.** A *thick tree map* is a continuous orientation-preserving map $F : \mathbb{T} \to \mathbb{T}$ such that:

1. $F$ is homeomorphism onto its image;
2. if $J$ is a junction of $\mathbb{T}$ then $F(J)$ is contained in a junction;
3. if $J$ and $J'$ are junctions such that $F(J) \subseteq J'$ then $F(\partial J \backslash \partial \mathbb{T}) \subseteq \partial J' \backslash \partial \mathbb{T}$;

4. if $X$ is an $n$-star connecting junctions $J_1, \ldots, J_k$, then $F(X)$ is an $n$-star connecting $F(J_1), \ldots, F(J_k)$.

Moreover, Figure 4.3 shows a thick tree map of a Hubbard tree that maps the critical junction in blue to the green junction; it maps the green junction to the red junction and the red junction to the yellow junction; and it pulls the yellow junction to the blue one.

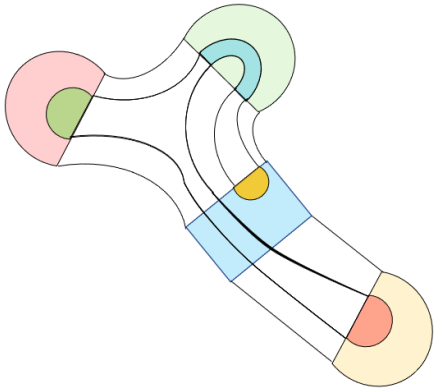

Figure 4.3: Thick tree map.

## 4.3 Tree-Like Train Tracks

**Definition 4.3.1.** We define a *tree-like train track* to be a family of vertices and curves embedded on a surface such that the following hold:

1. there are finitely many vertices of two types, called *switches* and *branch points*;
2. there are countably many curves of two types called *edges* and *loops*;
3. away from vertices, the curves are smooth and do not intersect;
4. the endpoints of each curve are vertices;
5. if the endpoints of a curve are the same point, the curve is called a *loop*. Otherwise, it is called an *edge*;
6. at branch points only edges can meet and at switches edges and loops can meet;
7. at each switch, countably many curves meet with a unique tangent line, with one edge entering from one direction and the remaining curves entering from the other direction;
8. the union of all edges is a topological tree.

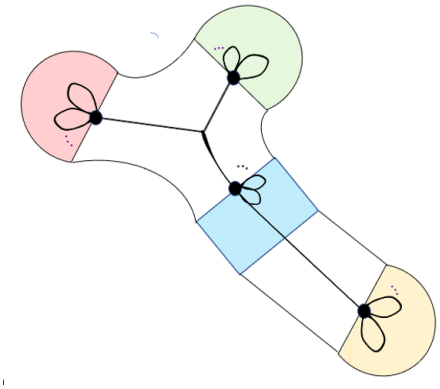

Figure 4.4: Tree-like train track.

# Chapter 5

# Constructing Generalized pseudo-Anosov Maps from Hubbard Trees

in this chapter, we will present a detailed proof of the main theorem.

## 5.1 Main Theorem

Consider a quadratic polynomial $f : \mathbb{C} \to \mathbb{C}$ with critical point $c_0$ of period $p$. Let $T$ be a Hubbard tree of $f$ such that it is non-degenerate, i.e. $c_0$ is not an endpoint of $T$. The critical point divides the tree into two connected components which we call *half-trees*. Denote the half-tree that contains $f(c_0)$ as the *upper branch* $B_u$ and the other one as the *lower branch* $B_l$.

**Definition 5.1.1.** The tree $T$ is said to be *crossing free* if the embedding of $T$ in the plane $\mathbb{C}$ is such that the image $f(B_l)$ of the lower branch can be isotoped, while fixing the endpoints of $T$, into a tree that does not intersect the interior $\overset{\circ}{f}(B_u)$ of the image of the upper branch.

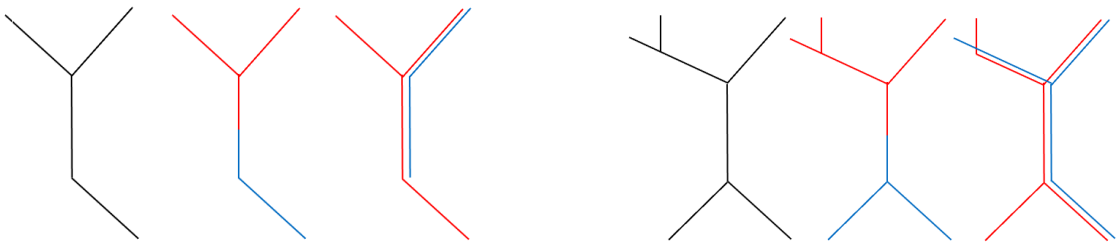

Crossing-free Hubbard tree. Hubbard tree with crossing.

Figure 5.1: Examples of Hubbard trees.

We will start with some lemmas about crossing-free Hubbard trees.

**Lemma 5.1.2.** *Let $T$ be a crossing-free non-degenerate Hubbard tree with a branch point $P$. Then the branch point $P$ cannot be mapped to a fixed branch point.*

*Proof.* Assume by contrary that there is a fixed branch point $P_0$ such that $f(P) = P_0$. Note that $P$ and $P_0$ cannot be in the same half-tree since the restriction of $f$ to each of the half-trees is injective. Looking at the images of the neighbourhoods of $P$ and $P_0$, we have the following:

- the images of neighbourhoods of $P$ and $P_0$ are neighbourhoods of $P_0$
- any sufficiently small neighbourhood of $P_0$ is homeomorphic to a star $S$ with $n > 2$ branches
- there is no homotopy that takes the star away from itself while staying in an $\epsilon$ neighbourhood of the tree.

This contradicts the crossing-free assumption. □

**Lemma 5.1.3.** *In a Hubbard tree, every branch point is pre-periodic. Moreover, if the tree is crossing free, then every pre-fixed branch point is fixed.*

*Proof.* Note that in any Hubbard tree, every branch point is mapped to a branch point. Since there are finitely many branch points, every branch point is pre-periodic. The second claim follows from Lemma 5.1.2. □

*Conjecture* 5.1.4. If the Hubbard tree is crossing-free, then there is only one branch point.

Now we will prove the first part of our main theorem.

**Theorem 5.1.5.** *Let $f$ be a post-critically finite quadratic polynomial and let $T$ be its Hubbard tree. If $(f, T)$ is crossing-free, then it is extendable to a generalized pseudo-Anosov homeomorphism.*

*Proof.* This is a proof by construction. Let $T$ be a crossing-free non-degenerate Hubbard tree. Let $c_0$ be the critical point with period $p$. Since $T$ is a non-degenerate Hubbard tree, then $c_0$ is located in the middle of $T$ between the upper branch $B_u$ and the lower branch $B_l$.

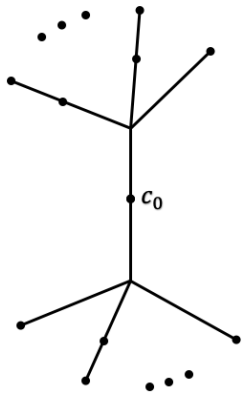


Figure 5.2

Since $T$ is a crossing-free Hubbard tree, then there exist:

$$\Phi_u : f(B_u) \times [0, 1] \to N_\epsilon(f(B_u)) \text{ defined by}$$

$$\Phi_u(p,t) = p, \quad \forall p \in \partial f(B_u), \quad \forall t,$$

and

$$\Phi_l : f(B_l) \times [0,1] \to N_\epsilon(f(B_l)) \text{ defined by}$$

$$\Phi_l(p,t) = p, \quad \forall p \in \partial f(B_l), \quad \forall t,$$

such that

$$\Phi_u(f(B_u)\backslash \partial f(B_u), 1) \cap \Phi_u(f(B_l)\backslash \partial f(B_l), 1) = \emptyset.$$

Now the construction will take the following steps:

**Step 1.** We thicken the tree $T$ into a thick tree $\mathbb{T}$ that consists of junctions $J$'s and sides $S$'s. Junctions are topologically discs that represent the critical orbit. So there are $p$ junctions in $\mathbb{T}$. In between junctions, there are sides $S$'s which are topologically rectangles such that the following holds:

- If the connected component $cc(\mathbb{T}\backslash\{J's, T\})$ contains a single edge of $T$ with no branch points, then $S = cc(\mathbb{T}\backslash\{J's, T\})$.
- If $cc(\mathbb{T}\backslash\{J's, T\})$ contains a branch point in $T_\theta$ of valence $n$, then we connect the branch point to each of the boundary component with lines $l_i$, for $1 \leq i \leq n$. Moreover, $cc(\mathbb{T}\backslash\{J's, T\})$ will contain $n$ sides $S_i$, $1 \leq i \leq n$ such that $S_i$ has $l_i \cup l_{i+1}$ as one side and a junction as the opposite side.

  Around an $n$-branch point, $n$ sides form an $n$-star

Note that in $\mathbb{T}$, there are $p$ junctions and $p + b - 1$ sides, where $b$ is the number of branch points.

Now define $\tilde{f} : f(T) \to N_\epsilon(f(T))$ by

$$\tilde{f}(x) = \begin{cases} \Phi_u(x,1) & \text{if } x \in f(B_u) \\ \Phi_l(x,1) & \text{if } x \in f(B_l) \end{cases}.$$

Starting with the thick tree $\mathbb{T}$, we embed the images $\tilde{f}(B_u)$ and $\tilde{f}(B_l)$ such that $J_{Red} = \tilde{f}(B_u) \cap J_{f(c_0)}$ and $J_{Blue} = \tilde{f}(B_l) \cap J_{f(c_0)}$ intersect at $f(c_0)$. We smoothen this point such that $J_{Red} \cup J_{Blue}$ is diffeomorphic to half a circle.

**Step 2.** We define a thick map $F : \mathbb{T} \to \mathbb{T}$ such that it satisfies the following:

1. $F(\mathbb{T}) \subseteq \mathbb{T}$.
2. The junction $J_{c_0}$ around the critical point $c_0$ is mapped homeomorphically into the junction $J_{c_1}$ around the critical value $c_1$ such that $F(J_{c_0}) \subseteq J_{c_1}$ and the two sides $J_{c_0,u}$ and $J_{c_0,l}$ of $\partial J_{c_0} \cap \overset{\circ}{\mathbb{T}}$ are mapped to disjoint segments of the one side of $\partial J_{c_1} \cap \overset{\circ}{\mathbb{T}}$ in the following way:
   - $F(J_{c_0,u})$ intersects $J_{Red}$ and $F(J_{c_0,l})$ intersects $J_{Blue}$,
   - $F : J_{c_0} \to F(J_{c_0}) \subseteq J_{c_1}$ is an embedding,
   - and the union $J_{Red} \cup J_{Blue}$ is contained in $F(J_{c_0})$.
3. Junctions that do not contain the critical point $c_0$ are mapped homeomorphically into junctions. More precisely, if $J_i$ contains $c_i$ with $i \in \{1, \ldots, p-1\}$, then $F(J_i)$ contains $f(c_i)$ and $F(J_i) \subseteq J_j$ for $j \in \{0, 1, \ldots, p-1\}$. There are three cases for such junctions:

**Case 1.** If end junction, end point of $T$, is mapped to end junction, then the boundary $\partial$ is mapped a boundary $\partial$, and the rest of the junction is embedded in the junction.

**Case 2.** If end junction is mapped to an inside junction, then the boundary $\partial$ is mapped the boundary part where it meets $\tilde{f}(B_\alpha)$.

**Case 3.** If an inside junction is mapped to an inside one, then the boundary $\partial$ sides will be mapped to the corresponding boundary sides such that they preserve the orientation of the original map.

4. Sides between junctions will be mapped as follows:

**Case 1.** If a side $S_i$ is connecting two junctions $J_m$ and $J_n$, then it is mapped to a side $F(S_i)$ that connects $F(J_m)$ and $F(J_n)$ such that:

- the inner boundary $\partial S_i \cap \overset{\circ}{\mathbb{T}}$ is mapped to $\partial F(J_m) \cap \overset{\circ}{\mathbb{T}}$ and $\partial F(J_n) \cap \overset{\circ}{\mathbb{T}}$,
- the outer boundary $\partial S_i \backslash (\partial S_i \cap \overset{\circ}{\mathbb{T}})$ is mapped to disjoint arcs that connect the boundary parts of the images of the junctions accordingly,
- and $F(S_i)$ is a rectangle that is a neighbourhood of $\tilde{f}(f(S_i \cap T))$.

**Case 2.** Around an $n$-branch point, $n$ sides form an $n$-star

. An $n$-star is mapped to an $n$-star, specifically, $n$ sides are mapped to $n$ rectangles each of which has $F(\partial S_i \cap \partial J_i)$ as one side.

Let $T$ be a tree connecting the critical orbit and representing the Hubbard tree $T_\theta$. For each $S_i$ there is a homeomorphism $h_i : S_i \to [0,1] \times [0,1]$ with a rectangle so that $h_i(T \cap S_i) = \{\frac{1}{2}\} \times [0,1]$. That is the tree is sent to the middle horizontal line. Let $P : [0,1] \times [0,1] \to \{1/2\} \times [0,1]$ be defined as

$$P(x,y) = (\frac{1}{2}, y).$$

Define $\pi_i : S_i \to T \cap S_i$ on each $S_i$ to be given by

$$\pi_i = h_i^{-1} \circ P \circ h_i$$

Define a continuous map $\xi_j : J_j \to J_j$ on each junction to be

$$\xi_j = \pi_i \text{ on } \partial J_j \cap \partial S_i$$

for every side $S_i$ that intersects the junction $J_j$, and so that the restriction of $\xi_j$ to the interior $J_j \setminus \cup(\partial S_i)$ is a homeomorphism onto its image.

We define an isotopy map on $\mathbb{T}$ as follows:

$$\psi : \mathbb{T} \to \mathbb{T}$$

$$\psi(z) = \begin{cases} \pi_i(z) & \text{if } z \text{ is in the side } S_i \\ \xi_j(z) & \text{if } z \text{ is in the junction } J_j. \end{cases}$$

To keep track of the folding, we construct a tree-like train track as follows:

- First we let $\tau_0 = (B_u \cup B_l) \setminus \overset{\circ}{J_0}$ be the disconnected tree-like train track with switches that are located at the intersection of the tree $T$ and the boundary of the junction $\partial J_0$.

- Then, we apply the map $F$ to $\tau_0$.
- Apply $\psi$ to $F(\tau_0)$.
- Denote the resulting by $\tau_1$.
- Now we continue by applying $F$ to $\tau_1$ and repeat the above process.
- This way, we get;

$$\tau_0 \subset \tau_1 \subset \cdots \subset \cup \tau_i.$$

More precisely, let $\Phi : \mathbb{T} \to \mathbb{T}$ be defined as

$$\Phi = \psi \circ F.$$

Define $\tau_n = \Phi^n(\tau_0)$. Since $\tau_0 \subset \tau_1$, then $\tau_n \subset \tau_{n+1}$ $\forall n$. Let

$$\tau_\infty = \bigcup_{n=0}^{\infty} \tau_n.$$

Then by construction

$$\Phi(\tau_\infty) = \Phi(\bigcup_{n=0}^{\infty} \tau_n) = \bigcup_{n=0}^{\infty} \Phi(\tau_n) = \bigcup_{n=1}^{\infty} \tau_n = \tau_\infty.$$

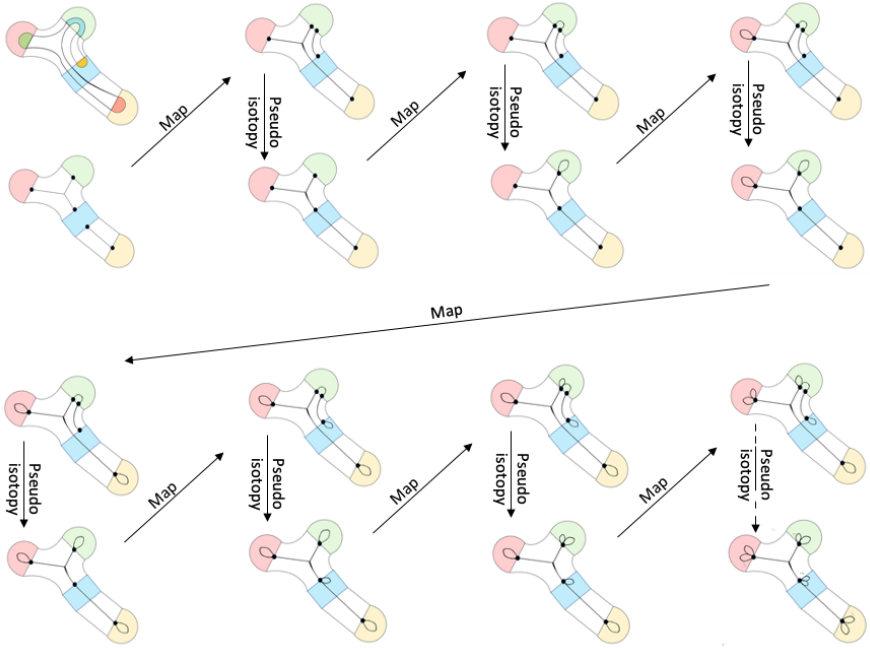


Figure 5.3: How to produce a tree-like train track using pseudo-isotopies.

Let $t_i = \pi(S_i),\ 1 \leq i \leq s$ be the edges of the tree-like train track $\tau_\infty$. Define a matrix $M = (m_{ij})$ where $m_{ij}$ equals the number of times $t_i$ crosses $\Phi(t_j)$ for $1 \leq i, j \leq s$.

Let $\lambda$ be the leading eigenvalue and $x = (x_1, \ldots, x_s)$ and $y = (y_1, \ldots, y_s)$ be the right- and left-eigenvalues corresponding to $\lambda$, respectively. Then we construct rectangles $R_i, 1 \leq i \leq s$, of dimensions $x_i \times y_i$. Then we glue these rectangles. To show that this gluing is possible, we will look at the various cases of the branch points. First we will consider the case where the valence is an odd number $n$. Then for the case of an even valence, we will consider the three options of the branch point, the case of a fixed branch point, the case of periodic branch point with period $k > 1$, and the case of pre-periodic branch point with pre-period $l > 1$.

The next lemma shows that it's possible to glue the rectangles around a branch point with odd valence.

**Lemma 5.1.6.** *Let $\tau$ be a tree-like train track with a branch point $p$ of valence $n$, where $n$ is odd. Let $R_i, i = 1, \ldots, n$, be $n$ rectangles constructed for the edges around the branch point $p$ in either a clockwise or counter-clockwise direction. Let $x_i$ and $y_i$ be the sides of $R_i$. Then we can glue all of $Y_i, i = 1, \ldots, n$, around the branch point such that each $y_i$ is divided into two subsegments $z_i$ and $w_i$, and $w_i$ is glued to $z_{i+1}$.*

*Proof.* We need to show that the gluing of the subsegments is possible. Let the rectangles $R_i, i = 1, \ldots, n$, be organized in a counter-clockwise order such that the sides $y_1, \ldots, y_n$ form an $n$-polygon. So we want to find if the following system has a well-defined solution:

$$\begin{aligned} z_1 + z_2 &= y_1 \\ z_2 + z_3 &= y_2 \\ &\vdots \\ z_n + z_1 &= y_n \end{aligned} \tag{5.1.1}$$

Since $n$ is odd: The above system of equations (5.1.1) has the augmented matrix

$$\begin{bmatrix} 1 & 1 & 0 & \ldots & & 0 \\ 0 & 1 & 1 & \ldots & & 0 \\ \vdots & & \ddots & & & \vdots \\ 0 & 0 & \ldots & 1 & 1 & 0 \\ 0 & 0 & \ldots & & 1 & 1 \\ 1 & 0 & \ldots & & 0 & 1 \end{bmatrix},$$

such that the following hold

$$\begin{bmatrix} 1 & -1 & \ldots & 1 & -1 & 1 \end{bmatrix} \begin{bmatrix} 1 & 1 & 0 & \ldots & & 0 \\ 0 & 1 & 1 & \ldots & & 0 \\ \vdots & & \ddots & & & \vdots \\ 0 & 0 & \ldots & 1 & 1 & 0 \\ 0 & 0 & \ldots & & 1 & 1 \\ 1 & 0 & \ldots & & 0 & 1 \end{bmatrix} = \begin{bmatrix} 2z_1 & 0 & \ldots & 0 \end{bmatrix}.$$

Hence we have

$$y_1 - y_2 + \cdots + y_{n-1} - y_n = 2z_1.$$

Since $z_1$ must be positive, we need the following condition to hold

$$y_1 + \cdots + y_{n-1} > y_2 + \cdots + y_n.$$

But this is true since $y_i > y_{i+1}, i = 1, \ldots, n-1$, given that $y_i = \lambda y_{i+1}$. This completes the proof. □

In the case of gluing the rectangles around a branch point with an even valence, the next lemma shows that it is possible for a fixed branch point.

**Lemma 5.1.7.** *Let $\tau$ be a tree-like train track with a fixed branch point $p$ of valence $n$. Let $R_i, i = 1, \ldots, n$, be $n$ rectangles constructed for the edges around the branch point $p$ in either a clockwise or counter-clockwise direction. Let $x_i$ and $y_i$ be the sides of $R_i$. Then we can glue all of $Y_i, i = 1, \ldots, n$, around the branch point such that each $y_i$ is divided into two subsegments $z_i$ and $w_i$, and $w_i$ is glued to $z_{i+1}$.*

*Proof.* Again here we need to show that the gluing of the subsegments is possible. Let the rectangles $R_i, i = 1, \ldots, n$, be organized in a counter-clockwise order such that the sides $y_1, \ldots, y_n$ form an $n$-polygon. So we want to find if the following system has a well-defined solution:

$$\begin{aligned} z_1 + z_2 &= y_1 \\ z_2 + z_3 &= y_2 \\ &\vdots \\ z_n + z_1 &= y_n \end{aligned} \tag{5.1.2}$$

Since $n$ is even, then the above system of equations (5.1.2) has the augmented matrix

$$\begin{bmatrix} 1 & 1 & 0 & \ldots & 0 \\ 0 & 1 & 1 & \ldots & 0 \\ \vdots & & \ddots & & \vdots \\ 0 & 0 & \ldots & 1 & 1 \\ 1 & 0 & \ldots & 0 & 1 \end{bmatrix},$$

with rank $n-1$. Hence, the $\dim(Ker) = 1$ with $(1, -1, \ldots, 1, -1)$ in the Kernel. That is

$$y_1 - y_2 + \cdots + y_{n-1} - y_n = 0. \tag{5.1.3}$$

Also, the Markov matrix of the system associated to the tree-like train track is given by the matrix

$$M = \left[\begin{array}{ccccc|c} 0 & 1 & 0 & \dots & 0 & \\ 0 & 0 & 1 & \dots & 0 & \\ \vdots & & \ddots & \ddots & \vdots & B \\ 0 & 0 & \dots & 0 & 1 & \\ 1 & 0 & \dots & 0 & 0 & \\ \hline & & A & & & C \\ & & & & & \end{array}\right],$$

where the upper left block is $n \times n$ coming from the half-tree that contains the branch point, say, the upper branch $B_u$. Then the block $C$ is coming from the other half-tree, in this case the lower branch $B_l$, say it's $m \times m$.

We claim that

$$Mv = -v \tag{5.1.4}$$

where $v = (1, -1, \dots, 1, -1, 0, \dots, 0)$ is an eigenvector associated to the eigenvalue $-1$.

The claim is true because block $A$ has all zeros except for the first row which is given exactly by $\begin{bmatrix} 1 & 1 & 0 & \dots & 0 \end{bmatrix}$. In fact, the rows of block $A$ represent all the edges that are disjoint from the branch point. Block $A$ contains ones only on places representing sides containing a pre-image $q \neq p$ of the branch point. Since the tree-like train track has a fixed branch point then by Lemma 5.1.2, there is no other branch point that's mapped to the fixed point. Hence the other pre-image $q$ is not a branch point. So $q$ lies on some edge $e_j, j > n$ in the lower branch. The edge $e_j$ maps to the union of two edges containing the critical point, and since the tree is crossing free, the two edges are consecutive. This gives rise to consecutive ones in row $j$ of block $A$. This proves the claim.

On the other hand, the transpose is given by the matrix

$$M^\intercal = \left[\begin{array}{ccccc|c} 0 & 0 & 0 & \dots & 1 & \\ 1 & 0 & 0 & \dots & 0 & \\ \vdots & \ddots & \ddots & & \vdots & A \\ 0 & 0 & \dots & 0 & 0 & \\ 0 & 0 & \dots & 1 & 0 & \\ \hline & & B & & & C \\ & & & & & \end{array}\right].$$

Let $\lambda$ be the leading eigenvalue for $M^\intercal$ and since $(y_1, \dots, y_{n+m})$ is the associated eigenvector, then we have

$$M^\intercal y = \lambda y \tag{5.1.5}$$

i.e.

$$\left[\begin{array}{ccccc|c} 0 & 0 & 0 & \dots & 1 & \\ 1 & 0 & 0 & \dots & 0 & \\ \vdots & \ddots & \ddots & & \vdots & A \\ 0 & 0 & \dots & 0 & 0 & \\ 0 & 0 & \dots & 1 & 0 & \\ \hline & & B & & & C \\ & & & & & \end{array}\right] \begin{bmatrix} y_1 \\ y_2 \\ \vdots \\ y_n \\ \vdots \\ \vdots \\ y_{n+m} \end{bmatrix} = \lambda \begin{bmatrix} y_1 \\ 2 \\ \vdots \\ y_n \\ \vdots \\ \vdots \\ y_{n+m} \end{bmatrix}$$

(5.1.4) and (5.1.5) give the following

$$\begin{aligned} v^\intercal(M^\intercal y) &= v^\intercal(\lambda y) \\ (Mv)^\intercal y &= \lambda(v^\intercal y) \\ -\langle v, y\rangle &= \lambda\langle v, y\rangle, \end{aligned}$$

which implies

$$(\lambda + 1)\langle v, y\rangle = 0.$$

Since $\lambda \neq -1$, we get

$$\langle v, y\rangle = 0. \tag{5.1.6}$$

This gives what we wanted to show as in (5.1.3). □

The following lemma shows that the gluing is possible in the case of a periodic branch point with period $k > 1$.

**Lemma 5.1.8.** *Let $\tau$ be a tree-like train track with a periodic branch point $p$ of valence $n$ and period $k > 1$. Let $R_i, i = 1, \dots, n$, be $n$ rectangles constructed for the edges around the branch point $p$ in either a clockwise or counter-clockwise direction. Let $x_i$ and $y_i$ be the sides of $R_i$. Then we can glue all of $Y_i, i = 1, \dots, n$, around the branch point such that each $y_i$ is divided into two subsegments $z_i$ and $w_i$, and $w_i$ is glued to $z_{i+1}$.*

*Proof.* Since $p$ is a periodic branch point of valence $n$ and period $k$, then this part of the Hubbard tree will consist of $k$ branches as shown in Figure 5.4. The edges around $p$ are denoted by $e_1, \dots, e_n$ in the counter-clockwise direction where $e_1$ is the edge connecting the branch point $p$ to other part of the Hubbard tree. Call the branch point $p$ with the edges $e_1, \dots, e_n$ a $p$-star denoted by $S_p$. We look at the dynamics of the $k$-th iteration of the map $f$ on all edges $e_i$ of the Hubbard tree $T$ and choosing the ones intersecting the $p$-star. This gives the following:

$$\{f^k(e_1), f^k(e_2), \dots, f^k(e_n)\} = \{e_1, e_2, \dots, e_n\}$$

If there is an edge $e_j$ in the Hubbard tree $T$ such that $f^k(e_j)$ intersects the $p$-star, then the intersection $f^k(e_j) \cap S_p = e_i \cup e_{i+1}$ for some $i = 1, \dots, n-1$. This is because of the condition that the Hubbard tree $T$ is crossing free. This will show in the Markov matrix for $f^k$ as an upper block which is an $n \times n$ matrix as in the proof of Lemma 4 and all rows in block $B$ are zeroes except for some with

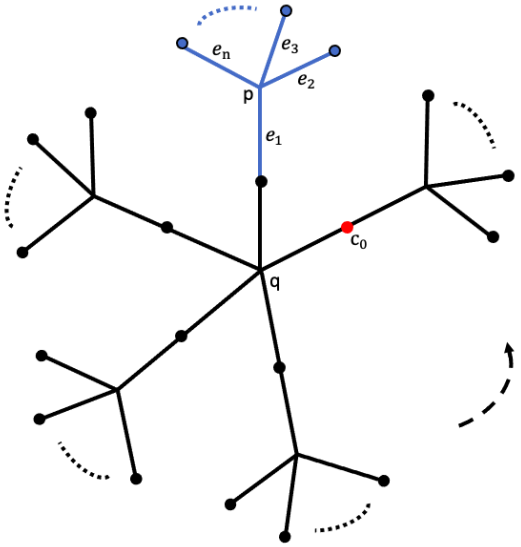


Figure 5.4: A periodic branch point $p$ of valence $n$ and period $k$.

consecutive ones.

$$\left[\begin{array}{ccccc|c} 0 & 0 & 0 & \dots & 1 & \\ 1 & 0 & 0 & \dots & 0 & \\ \vdots & \ddots & \ddots & & \vdots & A \\ 0 & 0 & \dots & 0 & 0 & \\ 0 & 0 & \dots & 1 & 0 & \\ \hline & & B & & & C \\ & & & & & \end{array}\right]$$

Following the same argument in Lemma 4, we get the result. This completes the proof.

□

**Lemma 5.1.9.** *Let $\tau$ be a tree-like train track with a pre-periodic branch point $p$ of valence $n$ and period $k > 1$. Let $R_i, i = 1, \dots, n$, be $n$ rectangles constructed for the edges around the branch point $p$ in either a clockwise or counter-clockwise direction. Let $x_i$ and $y_i$ be the sides of $R_i$. Then we can glue all of $Y_i, i = 1, \dots, n$, around the branch point such that each $y_i$ is divided into two subsegments $z_i$ and $w_i$, and $w_i$ is glued to $z_{i+1}$.*

*Proof.* Since $p$ is pre-periodic, then there is a number $l$ such that $f^l(p)$ is periodic and by the last Lemma, hence the gluing is possible for $f^l(p)$. Then we pull back and that will give the result. □

The last three lemmas showed that the gluing of the $n$-rectangles around the branch point $p$ is possible.

So now we organize all rectangles following the tree-like train track such that the edges of the tree-like train track represent the $x$-direction of the rectangles. Then we glue each two adjacent rectangles in the $y$-direction. For those $n$-rectangles around the branch point $p$, the gluing is done in the way described by the previous Lemmas such that a hyperbolic angle is formed. If there is no

branch point, then we glue the two rectangles such that they align in the $x$-direction on the side opposite of the loops as in Figure 5.5.

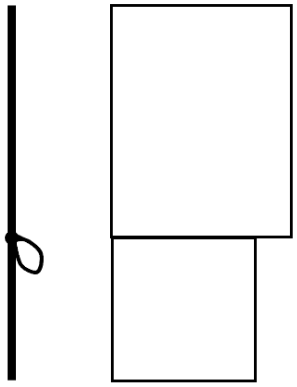

Figure 5.5: Aligning rectangles according to loops direction.

Let $\mathcal{R}$ be the union of all the rectangles $R_i$. Define $H : \mathcal{R} \to \mathcal{R}$ by

$$H(R_i) = \tilde{R}_j$$

such that the following hold:

- $\tilde{R}_j$ has dimension $x_i\lambda \times y_i\lambda^{-1}$,
- $\tilde{R}_j$ is located in the part of $\mathcal{R}$ that corresponds to the image $F(e_i)$ in $F(\tau_\infty)$, say $\tilde{R}_j \subseteq \cup R_k$ for some $k$, and
- $\tilde{R}_j$ align in the $x$-direction with $\cup R_k$ on the side following the image $F(\tau_\infty)$ of the tree-like train track.

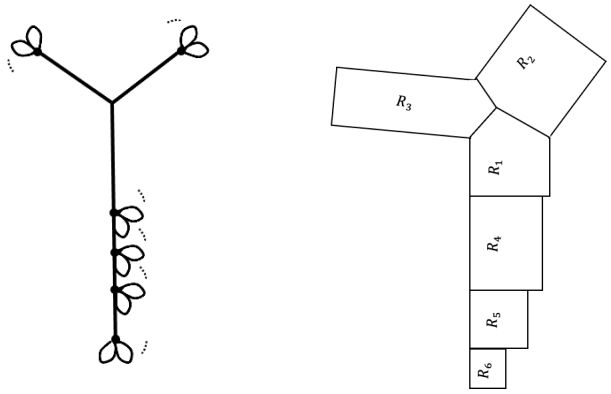


Figure 5.6: Gluing all the rectangles using the tree-like train track to get the surface $\mathcal{R}$.

$H$ acts homeomorphically on $\mathcal{R}\backslash(\partial\mathcal{R} \cup L_0)$ where $L_0$ is the side representing the critical point. We then glue the $x$-direction of the boundary $\partial\mathcal{R}$ by the following steps:

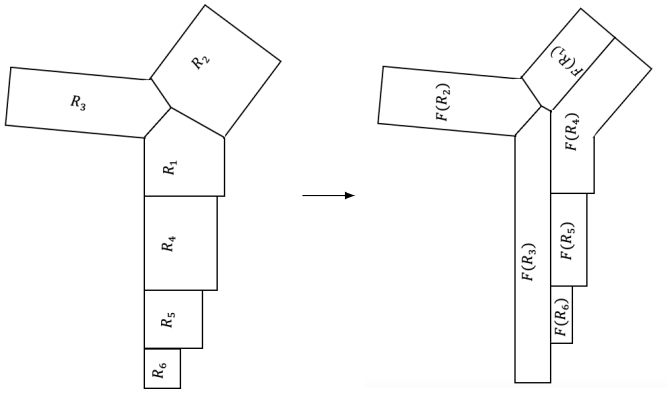


Figure 5.7: Applying the induced map $H$ on $\mathcal{R}$.

1. first identify the pre-images of each segment in the $x$-direction of the image of the boundary $H(\partial\mathcal{R})$,
2. then glue the remaining parts of the $x$-direction of the boundary $\partial\mathcal{R}$ by following the identifications in step 1 and pull-back to the pre-images.
3. repeat step 2 until all the $x$-direction of the boundary $\partial\mathcal{R}$ are identified.

Last we identify the rest of the $y$-direction of the boundary $\partial\mathcal{R}$, which represent the loops in the tree-like train track, as follows:

- starting from the side of the first formed loop, we pinch the side and identify the two sides of the pinch;
- then we continue with a set of identifications by pinching the remaining part of the side where each pinch represents a loop;
- since there are infinite loops, then there will be a set of infinite pinching or identifications;
- to decide the exact points of the side where the identifications take place we use the following equation

$$\sum_{n=0}^{\infty} \lambda^{-np} y_0 = y$$

where $y$ is the length of the side, $y_0$ is the length of the first identification, $\lambda$ is the leading eigenvalue, and $p$ is the period of the critical point.

We now need to show that the infinite singularities, occurring from the boundary identifications, accumulate at finitely many points. First, let us take care of the singularities formed from the loops in the tree-like train track. Since $f$ is a post-critically finite map, then there are finite number of connected segments $\tilde{S}_i$ in the boundary $\partial\mathcal{R}$ with loops. Each segment $\tilde{S}_i$ has infinite singularities. WLOG, let $\tilde{S}_i$ be a side of length $y$, and let's parameterize it as an interval $\tilde{S}_i = [0, y]$ such that 0 corresponds to the side of $\tilde{S}_i$ that the first singularity is located. Thus the singularities will be located in the interval $[0, y_i]$ exactly at the points

$$\frac{y_i}{2},\ y_i + \frac{y_i}{2\lambda^p},\ y_i + \frac{y_i}{2} + \frac{y_i}{2\lambda^{2p}},\ \cdots$$

Since

$$\lim_{n\to\infty} \frac{y_i}{2\lambda^{np}} = 0,$$

then the singularities on $\tilde{S}_i$ accumulate at the point

$$y_i + \frac{y_i}{\lambda^p} + \frac{y_i}{\lambda^{2p}} + \ \cdots = y.$$

Now we look at the singularities in the $x$-direction. Similarly, for the singularities in the $x$-direction, there is at most one limit point on each side of the thickened tree. To show this, we start with the sides on the boundary of $\mathcal{R}$ that get mapped to the interior $\overset{\circ}{\mathcal{R}}$, and identify them if they have the same image. After that, we iteratively pull back these identifications to produce all the identifications. This shows that the resulting map $\phi$ in the quotient is a generalized pseudo-Anosov. □

**Definition 5.1.10.** Let $\varphi : S \to S$ be a generalized pseudo-Anosov homeomorphism of a surface $S$, let $\mathcal{F}$ be one of its invariant foliations, and let $f : T \to T$ be a Hubbard tree of a post-critically finite quadratic polynomial. Let $T_0$ be the tree $T$ minus the endpoints. Suppose the following holds:

1. there exists an open, connected, dense subset $S_0$ of $S$;
2. the quotient map, given by collapsing each leaf of the restriction of $\mathcal{F}$ to $S_0$, yields a surjective, continuous map $\pi : S_0 \to T_0$;
3. the following diagram commutes:

$$\begin{array}{ccc} S_1 & \xrightarrow{\varphi} & S_0 \\ {\scriptstyle\pi}\downarrow & & \downarrow{\scriptstyle\pi} \\ T_1 & \xrightarrow{f} & T_0 \end{array}$$

   where $S_1 := \varphi^{-1}(S_0)$ and $T_1 := f^{-1}(T_0)$.

Then we say that $\varphi$ is an *extension* of $f$.

Now we will prove the converse of theorem 2, that is the second part of the main theorem:

**Theorem 5.1.11.** *If $\varphi$ is a generalized pseudo-Anosov map that is an extension of a non-degenerate Hubbard tree $T$ then $T$ is crossing free.*

*Proof.* Since $\varphi$ is a generalized pseudo-Anosov map that is an extension of a non-degenerate Hubbard tree $T$, then the following diagram commutes:

$$\begin{array}{ccc} S_1 & \xrightarrow{\varphi} & S_0 \\ {\scriptstyle\pi}\downarrow & & \downarrow{\scriptstyle\pi} \\ T_1 & \xrightarrow{f} & T_0 \end{array}$$

where $\pi : S_0 \to T_0$ is the quotient map given by collapsing each leaf of one of the invariant foliations $\mathcal{F}$ of $\varphi$ to a point, and $f : T \to T$ is a continuous map. In order to show that $T$ is crossing-free, we need to show that the embedding of $T_0$ in $S_0$ has the following property: the images $f(B_u)$ and

$f(B_l)$ of the upper and lower branches can be isotoped, while fixing the endpoints of $T$, into two trees with disjoint interiors.

To show this, first we define $i : T_0 \to S_0$ such that $\pi \circ i = id_{T_0}$. Consider $T = B_u \cup B_l$. Let $\tilde{B}_u = i(B_u \cap T_0), \tilde{B}_l = i(B_l \cap T_0)$. Since $\varphi$ is a homeomorphism on $S$, then $\varphi(\tilde{B}_u \backslash \{c_0\}) \cap \varphi(\tilde{B}_l \backslash \{c_0\}) = \phi$. Let $\tilde{T} = i(T_0)$. Let $\tilde{c_0} = i(c_0)$ and $\tilde{c_1} = \varphi(\tilde{c_0})$. Let $d_{\mathcal{F}}(x, y)$ be the distance between the leaves of $\mathcal{F}$ containing $x$ and $y$.

Since $S_0$ can be embedded in the plane, we can use coordinates of the plane to define a homotopy as follows:

$$H : \tilde{T} \times [0, 1] \to S_0 \text{ given by}$$

$$H(x, 0) = \tilde{f}(x) = i(f(\pi(x))) \text{ and } H(x, 1) = d_{\mathcal{F}}(x, \tilde{c_1})\varphi(x) \text{ for all } x \in \tilde{T},$$

and

$$H(x, t) = (1 - t)H(x, 0) + t\ H(x, 1),\ t \in [0, 1].$$

Since $S_0$ can be embedded in the plane $\mathbb{C}$, then $H$ is a homotopy in $\mathbb{C}$. We can extend the homotopy to the endpoints of $T$ and note that it induces an isotopy on the upper and lower branches because by definition, at each time $t$ every leaf will contain exactly one point of $H(\tilde{B}_u, t)$ and the same hold for the $H(\tilde{B}_l, t)$. Now we obtained the isotopy in the definition of the crossing-free.

That completes the proof.

□

# Chapter 6

# Examples

In this chapter, we will give examples of both crossing-free Hubbard tree and a Hubbard tree with crossing. For the former, we will show in details how we can construct the generalized pseudo-Anosov.

## 6.1 An example of a crossing-free Hubbard tree

In this section, we will show with an example how to construct a pseudo-Anosov map from a crossing-free Hubbard tree.

Recall example 2.5.5 in section 2.5, where $f$ is a post-critically finite quadratic polynomial with the characteristic angle $\theta = \frac{1}{5}$. Since the Hubbard tree $T$ is crossing-free, then by Theorem (5.1.5) it is extendable to a generalized pseudo-Anosov homeomorphism.

Now using the Markov matrix, we will construct the strips as follows: The leading eigenvalue of

$$M = \begin{bmatrix} 0 & 1 & 0 & 0 \\ 0 & 0 & 1 & 0 \\ 1 & 0 & 0 & 1 \\ 1 & 1 & 0 & 0 \end{bmatrix}$$

is $\lambda = 1.39534$ with eigenvector $(0.582522, 0.812815, 1.13415, 1)$. We also have the leading eigenvalue of the transpose

$$M^{\intercal} = \begin{bmatrix} 0 & 0 & 1 & 1 \\ 1 & 0 & 0 & 1 \\ 0 & 1 & 0 & 0 \\ 0 & 0 & 1 & 0 \end{bmatrix}$$

is $\lambda = 1.39534$ with eigenvector $(1.71667, 1.94697, 1.39534, 1)$. Normalizing these right- and left-eigenvectors we get:

$$x = (0.16504438, 0.23029267, 0.32133565, 0.28332729)$$

and

$$y = (0.28332657, 0.32133626, 0.23029289, 0.16504428).$$

Now we construct the rectangular strips of dimensions $x_i \times y_i$ as in the following Figure 6.1:

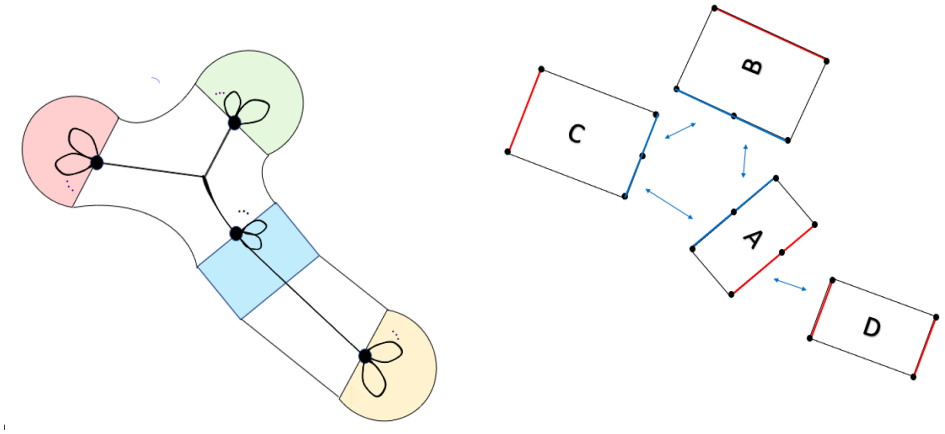


Figure 6.1: Constructing rectangular strips.

### 6.1.1 Rectangle decomposition of a surface

After identifying the sides and applying the map we get the following:

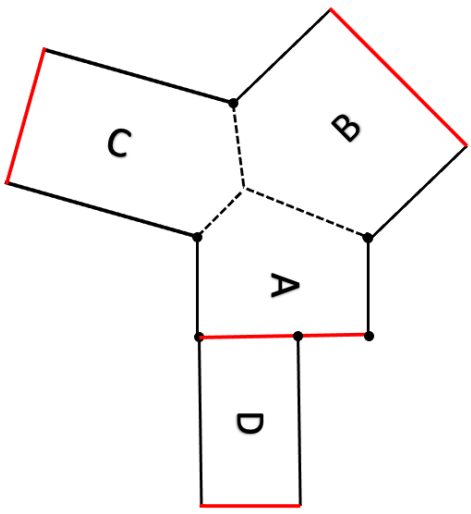


The rectangle decomposition of a surface from the train track.

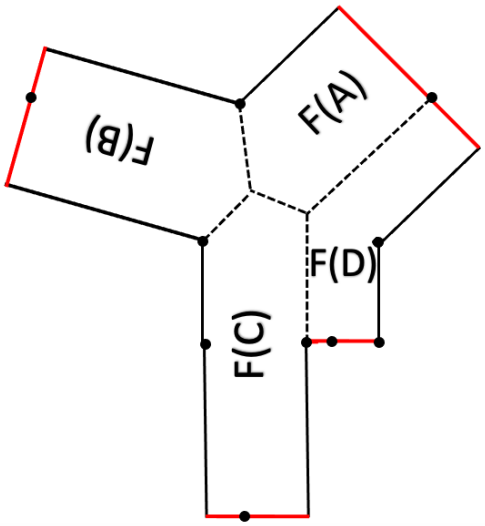


The rectangle decomposition of the surface after applying the map.

Figure 6.2

Using the $x$-dimensions of $A, B, C$, and $D$ from the picture in Figure 6.2, we will show that the identifications presented in Figure 6.3 is correct. Since $C$ is mapped to $A$ and $D$, and from Figure 9 we find that there will be an identification between $A$ and an equal part of $D$. We represented this as red arrows left of $C$ in Figure 6.3. The remainder of $D$ that is $D - A$ from Figure 6.2, will be identified with an equal part of $C$. These are shown as yellow arrows on top of $C$ and $B$ in Figure 6.3. In the following calculations we refer to the parts from Figure 6.2 and the identifications in Figure 6.3:

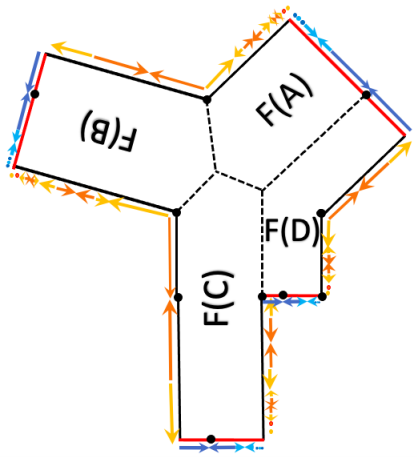


Figure 6.3: Identifying the sides.

$$
\begin{aligned}
C =&(D-A)+F^{-4}(A+D+(D-A))+F^{-4}(F^{-4}(A+D+(D-A)))+\dots\\
=&D-A+F^{-4}(2D)+F^{-4}(F^{-4}(2D))+\dots\\
=&D-A+2D\sum_{n=1}^{\infty}(\frac{1}{\lambda^4})^n\\
=&D-A+2D(\frac{1}{1-\frac{1}{\lambda^4}}-1)\\
=&D-(\lambda C-D)+2D(\frac{1}{\lambda^4-1})\\
=&-\lambda C+2D(\frac{1}{\lambda^4-1}+1)\\
=&-\lambda C+2D(\frac{\lambda^4}{\lambda^4-1})\\
=&\frac{-\lambda C(\lambda^4-1)+2D\lambda^4}{\lambda^4-1}\\
=&\frac{-\lambda C(\lambda^4-1)+2(\lambda C-A)\lambda^4}{\lambda^4-1}\\
=&\frac{-\lambda C(\lambda^4-2\lambda+1)}{\lambda^4-1}
\end{aligned}
$$

Notice that with $\lambda = 1.39534$, we have

$$\frac{-\lambda C(\lambda^4-2\lambda+1)}{\lambda^4-1} \approx C$$

Similarly, we find that all the identifications in Figure 6.3 match the lengths of the $x$-coordinates of the strips.

## 6.2 An example of a Hubbard tree with crossing

Let $g$ be a quadratic polynomial with the characteristic angle $\theta = \frac{3}{16}$. The critical point $c_0$ is pre-periodic as can be seen in Figure 6.4. Figure 6.5 shows the thick tree on the left and the thick tree map on the right. Notice that there is a crossing ocurring in the thick tree map which corresponds to a crossing in it's Hubbard tree. This crossing is the place where the construction of the tree-like train track fails.

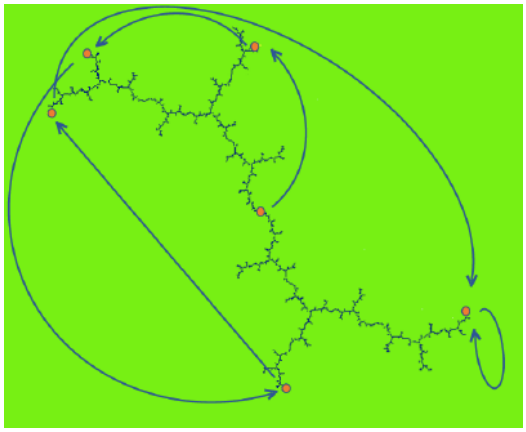

Hubbard tree of PCF polynomial with angle $\frac{3}{16}$.

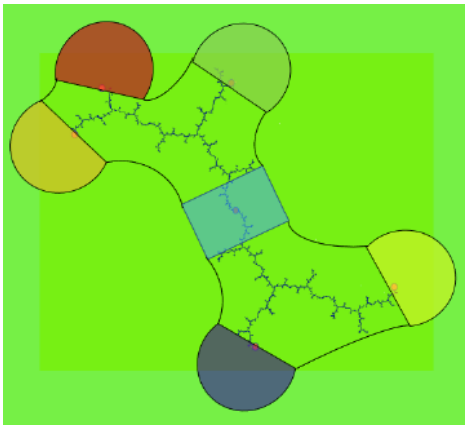

Thickening the Hubbard tree.

Figure 6.4

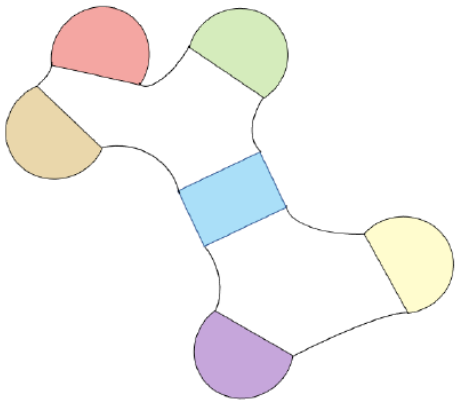

Thick Hubbard tree.

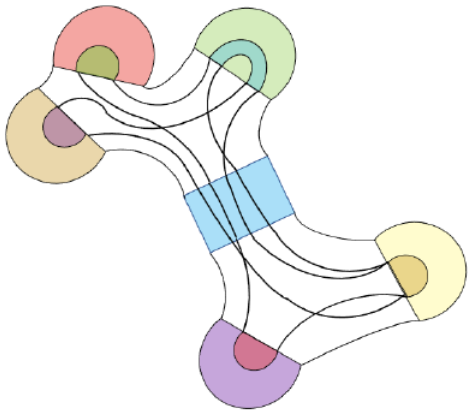

Thick tree map showing crossing.

Figure 6.5

# Bibliography


[BCK21] Hyungryul Baik, Inhyeok Choi, Dongryul M. Kim, *Topological entropy of pseudo-Anosov maps from a typical Thurston's construction*, arXiv:2006.10420v4 [math.DS] 17 Feb 2021.

[BdCH24] Philip Boyland, André de Carvalho, Toby Hall, *The Dynamics of Measurable Pseudo-Anosov Maps*, arXiv:2306.16841v2 [math.DS] 23 July 2024.

[BH95] Mladen Bestvina, Michael Handel, *Train-tracks for surface homeomorphisms*, Topology 34 (1995) 109–140 MR1308491.

[BH92] Mladen Bestvina, Michael Handel, *Train Tracks and Automorphisms of Free Groups*, Annals of Mathematics, Jan., 1992, Second Series, Vol. 135, No. 1 (Jan., 1992), pp. 1-51.

[BLMW22] James Belk, Justin Lanier, Dan Marglit, and Rebecca R. Winarski, *Recognizing topological polynomials by lifting trees*, Duke Math. J. 171 (2022), no. 17, 3401-3480.

[BRW15] HYUNGRYUL BAIK, AHMAD RAFIQI, CHENXI WU, *Constructing pseudo-Anosov maps with given dilatations*, arXiv.org/pdf/1411.1385v2 [math.GT] 25 Feb 2015.

[Do82] Adrien Douady and John Hamal Hubbard, *Itération des polynômes quadratiques complexes*, C. R. Acad. Sci. Paris S´er. I Math. 294 (1982), no. 3, 123–126. MR 651802.

[Do93] Adrien Douady, *Descriptions of compact sets in C*, in: *Topological Methods in Modern Mathematics*, Stony Brook, NY, 1991, Publish or Perish, Houston, 1993, pp.429–465.

[DDTKOPR23] Ryan Dickmann, George Domat, Thomas Hill, Sanghoon Kwak, Carlos Ospina, Priyam Patel, Rebecca Rechkin, *Thurston's Theorem: Entropy in Dimension One*, arXiv:2209.15102v2 [math.GT] 7 Apr 2023.

[dC05] André de Carvalho, *Extensions, quotients and generalized pseudo-Anosov maps*, In Graphs and patterns in mathematics and theoretical physics, volume 73 of Proc. Sympos. Pure Math., pages 315 338. Amer. Math. Soc., Providence, RI, 2005.

[dCH04] André de Carvalho and Toby Hall, *Unimodal generalized pseudo-Anosov maps*, Geom. Topol., 8:1127 1188, 2004.

[DH84] Adrien Douady, John H. Hubbard, *Etude dynamique des polynômes complexes*, Publications Mathématiques d'Orsay 84, Université de Paris-Sud, Département de Mathématiques, Orsay, 1984.

[Di24] Inti Cruz Diaz, *An Algorithmic Classification of Generalized Pseudo-Anosov Homeomorphisms via Geometric Markov Partitions*, arXiv:2405.07954v1 [math.DS] 13 May 2024.

[FLP12] Albert Fathi, Francois Laudenbach, Valentin Poénaru, *Thurston's Work on Surfaces*, translated by Djun Kim and Dan Margalit. p. cm. (Mathematical notes ; 48) (2012) ISBN 978-0-691-14735-2 (pbk.)

[FM12] Benson Farb, Dan Margalit, *A primer on mapping class groups*, (2012) by Princeton University Press, ISBN 978-0-691-14794-9.

[Fa22] Ethan Farber, *Constructing pseudo-Anosovs from expanding interval maps*, arXiv:2101.01721v3 [math.DS] 17 Feb 2022.

[Fr85] David Fried, *Growth rate of surface homeomorphisms and flow equivalence*, Ergodic Theory Dynam. Systems, 5(4):539 563, 1985.

[Ha94] Toby Hall, *The creation of horseshoes*, Nonlinearity, 7(3):861 924, 1994.

[HRS19] John Hubbard, Ahmad Rafiqi and Tom Schang, *Constructing pseudo-Anosov Maps from Permutations and Matrices* ,arXiv:1902.07440v3 [math.DS] 20 Jun 2019.

[Lu97] Feng Luo, *A presentation of the mapping class groups*, Mathematical Research Letters, 4 (1997), 735-739.

[LTW21] Kathryn Lindsey, Giulio Tiozzo, Chenxi Wu, *Master teapots and entropy algorithms for the Mandelbrot set*, arXiv:2112.14590 [math.DS] 29 Dec 2021.

[Mi90] John Milnor, *Dynamics in One Complex Variable*, Introductory Lectures (Partially revised version of 9-5-91) Institute for Mathematical Sciences, SUNY, Stony Brook, NY, 1990.

[Mi95] John Milnor, *Periodic Orbits, External Rays and the Mandelbrot set: an expository account*, 2000, Geometrie complexes at systemes dynamiques (Orsay, 1995), pp. xiii, 277-333.

[Pe88] Robert C. Penner, *A construction of pseudo-Anosov homeomorphisms*, Trans. Amer. Math. Soc. 310 (1988) 179–197.

[PH91] Robert C. Penner, John L. Harer, *Combinatorics of Train Tracks*, (AM-125), vol. 125 (1991), annals of Mathematics Studis.

[Sc04] Dierk Schleicher, *On Fibers and Local Connectivity of Mandelbrot and Multibrot Sets*, Lapidus, Frankenhuysen (eds), a Mandelbrot Jubilee. Proc Symp Pure Math 72 (2004), 477-507.

[Sc00] Dierk Schleicher, *Rational Parameter Rays of the Mandelbrot Set*, Asterisque 261 (2000), 409-447.

[SS15] Hyunshik Shin, Balázs Strenner, *Pseudo-Anosov mapping classes not arising from Penner's construction*, Geometry & Topology 19 (2015), no. 6, 3645–3656.

[Th88] William P. Thurston, *On the geometry and dynamics of diffeomorphisms of surfaces*, Bull. Amer. Math. Soc. (N.S.) 19 (1988), no. 2, 417–431.

[Th97] William P. Thurston, *Three-Dimensional Geometry and Topology VOLUME 1*, edited by Silvio Levy. p. em. - Princeton Mathematical Series 35, Princeton University Press, Princeton, New Jersey, 1997, pp. 1–328.

[Th09] William P. Thurston, *On the geometry and dynamics of iterated rational maps*, in: D. Schleicher, N. Selinger (Eds.), Complex Dynamics, A.K. Peters, Wellesley, MA, 2009, pp.3–137.

[Th14] William P. Thurston, *Entropy in dimension one*, in *Frontiers in complex dynamics*, volume 51 of Princeton Math. Ser., pages 339-384. Princeton Univ. Press, Princeton, NJ, 2014.

[TBGHLLT22] William P. Thurston, Hyungryul Baik, Yan Gao, John H. Hubbard, Tan Lei, Kathryn A. Lindsey, Dylan P. Thurston, *Degree-d-invariant laminations*, in *Collected works of William P. Thurston with commentary. Vol. III. Dynamics, computer science and general interest*, 223–289, Amer. Math. Soc., Providence, RI, 2022.

[Ti15] Giulio Tiozzo, *Topological entropy of quadratic polynomials and dimension of sections of the Mandelbrot set*, Advances in Mathematics 273 (2015), 651-715.

[Ti16] Giulio Tiozzo, *Continuity of core entropy of quadratic polynomials*, Invent. Math. 203 (2016), no. 3,8 91-921.